J|A|C|S ARTICLES

Published on Web 12/15/2009

Electronic Properties of Pentacene versus Triisopropylsilylethynyl-Substituted Pentacene: Environment-Dependent Effects of the Silyl Substituent

Olga Lobanova Griffith,[†] John E. Anthony,[‡] Adolphus G. Jones,[‡] and Dennis L. Lichtenberger*,[†]

Department of Chemistry and Biochemistry, The University of Arizona, Tucson, Arizona 85721, and Department of Chemistry, University of Kentucky, Lexington, Kentucky 40506-0055

Received August 14, 2009; E-mail: dlichten@email.arizona.edu

Abstract: Energy measures of the intra- and intermolecular electronic effects of triisopropylsilylethynyl substitution on pentacene have been obtained from the combination of closely related gas phase and solid phase ultraviolet photoelectron spectroscopy (UPS) measurements along with solution electrochemical measurements. The results show that the shift to lower ionization energy that is expected with this substitution and observed in the gas phase measurements becomes negligible in solution and is even reversed in the solid phase. The principles that emerge from this analysis are supported by electronic structure calculations at the density functional theory level. The relation between the gas phase and solid phase UPS measurements illustrated here provides a general approach to investigating the electronic effects acting on molecules in the condensed phase, which in this case are greater than the direct substituent electronic effects within the molecule. Electronic properties such as lower ionization energies built into the single-molecule building blocks of materials and devices may be reversed in the solid state.

Introduction

Electronic devices based on organic semiconductors represent a leading next-generation device technology.[1−12] Pentacenes are attractive building blocks for molecular devices due to their inherent electronic properties, excellent film-forming characteristics, and the ability to adjust the electronic behavior required for a particular device.[13−27] The tuning of electronic properties, such as charge injection barriers, HOMO−LUMO gaps, charge transfer rates, and molecular ordering of pentacenes is accomplished by substitution with different functional groups. One of the most popular pentacene derivatives is triisopropylsilylethynyl-substituted (TIPS) pentacene which has properties appropriate for its use in thin-film transistors.[9,28−36] The TIPS substituent alters the *intra*molecular electronic structure and

[†] Department of Chemistry and Biochemistry, The University of Arizona.
[‡] Department of Chemistry, University of Kentucky.

(1) Anthony, J. E. *Angew. Chem., Int. Ed.* **2008**, *47*, 452.
(2) Allard, S.; Forster, M.; Souharce, B.; Thiem, H.; Scherf, U. *Angew. Chem., Int. Ed.* **2008**, *47*, 4070.
(3) *Physics of Organic Semiconductors*; Bruetting, W., Ed.; Wiley-VCH Verlag GmbH & Co. KGaA: Weinheim, Germany, 2005; p 536.
(4) Dimitrakopoulos, C. D.; Malenfant, P. R. L. *Adv. Mater.* **2002**, *14*, 99.
(5) Facchetti, A. *Mater. Today* **2007**, *10*, 28.
(6) Ito, K.; Suzuki, T.; Sakamoto, Y.; Kubota, D.; Inoue, Y.; Sato, F.; Tokito, S. *Angew. Chem., Int. Ed.* **2003**, *42*, 1159.
(7) Katz, H. E.; Bao, Z. *J. Phys. Chem. B* **2000**, *104*, 671.
(8) Kelley, T. W.; Muyres, D. V.; Baude, P. F.; Smith, T. P.; Jones, T. D. *Mater. Res. Soc. Symp. Proc.* **2003**, *771*, 169.
(9) Payne, M. M.; Parkin, S. R.; Anthony, J. E.; Kuo, C.; Jackson, T. N. *J. Am. Chem. Soc.* **2005**, *127*, 4986.
(10) Podzorov, V.; Sysoev, S. E.; Loginova, E.; Pudalov, V. M.; Gershenson, M. E. *Appl. Phys. Lett.* **2003**, *83*, 3504.
(11) Nakayama, Y.; Machida, S.; Minari, T.; Tsukagishi, K.; Noguchi, Y.; Ishii, H. *Appl. Phys. Lett.* **2008**, *93*, 173305–173311.
(12) Duhm, S.; Heimel, G.; Salzmann, I.; Glowatzki, H.; Johnson, R. L.; Vollmer, A.; Rabe, J. P.; Koch, N. *Nat. Mater.* **2008**, *7*, 326.
(13) Gruhn, N. E.; da Silva Filho, D. A.; Bill, T. G.; Malagoli, M.; Coropceanu, V.; Kahn, A.; Bredas, J. *J. Am. Chem. Soc.* **2002**, *124*, 7918.
(14) Ishii, H.; Sugiyama, K.; Ito, E.; Seki, K. *Adv. Mater.* **1999**, *11*, 605.
(15) Kahn, A.; Koch, N.; Gao, W. *J. Polym. Sci., Part B: Polym. Phys.* **2003**, *41*, 2529.
(16) Kakuta, H.; Hirahara, T.; Matsuda, I.; Nagao, T.; Hasegawa, S.; Ueno, N.; Sakamoto, K. *Phys. Rev. Lett.* **2007**, *98*, 247601/1.
(17) Kanjilal, A.; Ottaviano, L.; DiCastro, V.; Beccari, M.; Betti, M. G.; Mariani, C. *J. Phys. Chem. C* **2007**, *111*, 286.
(18) Kaur, I.; Jia, W.; Kopreski, R. P.; Selvarasah, S.; Dokmeci, M. R.; Pramanik, C.; McGruer, N. E.; Miller, G. P. *J. Am. Chem. Soc.* **2008**, *130*, 16274.
(19) Koch, N.; Vollmer, A.; Duhm, S.; Sakamoto, Y.; Suzuki, T. *Adv. Mater.* **2007**, *19*, 112.
(20) Lin, Y. -.; Gundlach, D. J.; Nelson, S. F.; Jackson, T. N. *Electron Device Lett., IEEE* **1997**, *18*, 606.
(21) Lin, Y.; Gundlach, D. J.; Nelson, S. F.; Jackson, T. N. *IEEE Trans. Electron Devices* **1997**, *44*, 1325.
(22) Mattheus, C. C.; de Wijs, G. A.; de Groot, R. A.; Palstra, T. T. M. *J. Am. Chem. Soc.* **2003**, *125*, 6323.
(23) Sakamoto, Y.; Suzuki, T.; Kobayashi, M.; Gao, Y.; Fukai, Y.; Inoue, Y.; Sato, F.; Tokito, S. *J. Am. Chem. Soc.* **2004**, *126*, 8138.
(24) Singh, T. B.; Meghdadi, F.; Guenes, S.; Marjanovic, N.; Horowitz, G.; Lang, P.; Bauer, S.; Sariciftci, N. S. *Adv. Mater.* **2005**, *17*, 2315.
(25) Watkins, N. J.; Yan, L.; Gao, Y. *Appl. Phys. Lett.* **2002**, *80*, 4384.
(26) Coropceanu, V.; Cornil, J.; Da Silva Filho, D. A.; Olivier, Y.; Silbey, R.; Bredas, J. *Chem. Rev.* **2007**, *107*, 926.
(27) Delgado, M. C. R.; et al. *J. Am. Chem. Soc.* **2009**, *131*, 1502.
(28) Anthony, J. E. *Funct. Org. Mater.* **2007**, 511.
(29) Anthony, J. E.; Brooks, J. S.; Eaton, D. L.; Parkin, S. R. *J. Am. Chem. Soc.* **2001**, *123*, 9482.
(30) Lobanova Griffith, O.; Gruhn, N. E.; Anthony, J. E.; Purushothaman, B.; Lichtenberger, D. L. *J. Phys. Chem. C* **2008**, *112*, 20518.
(31) Coropceanu, V.; Malagoli, M.; da Silva Filho, D. A.; Gruhn, N. E.; Bill, T. G.; Bredas, J. L. *Phys. Rev. Lett.* **2002**, *89*, 275503/1.
(32) Palilis, L. C.; Lane, P. A.; Kushto, G. P.; Purushothaman, B.; Anthony, J. E.; Kafafi, Z. H. *Org. Electron.* **2008**, *9*, 747.

10.1021/ja906917r

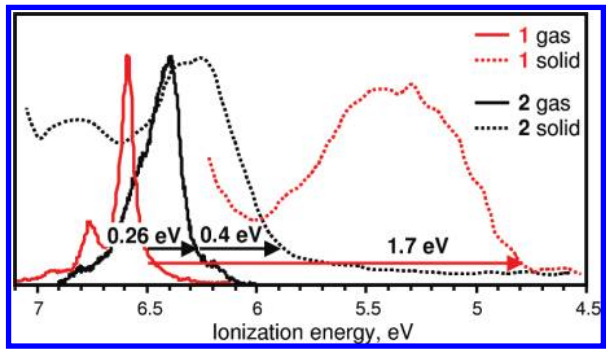

Figure 1. He I UPS: first ionization energy bands of pentacene 1 in red, and of TIPS pentacene 2 in black (solid lines − gas phase, dotted lines − solid phase).

*inter*molecular electronic interactions, thus leading to very different ionization energies, charge injection barriers, and

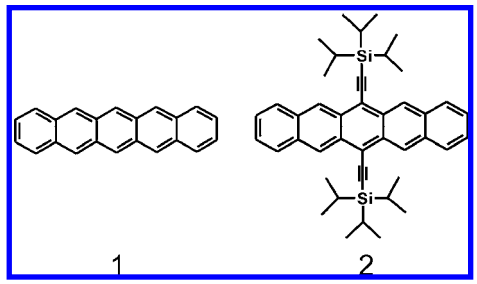

HOMO−LUMO energy gaps. A number of factors can influence these properties and their measures in the solid state, including interfacial and intermolecular morphologies[11] and molecular dipole orientations.[12]

In this work, we show how a direct energy measure of these intra- and intermolecular electronic effects can be obtained from the combination of closely related high-resolution gas phase and solid phase ultraviolet photoelectron spectroscopy (UPS) measurements. It is especially interesting that in this case the *inter*molecular effects (primarily polarization effects in the solid state) have a greater influence on the electronic properties of the material than the direct *intra*molecular electronic interactions of these substituents on the pentacene building blocks. These results are further clarified by electrochemical measurements and first-principles quantum-mechanical calculations.

Results and Discussion

Gas-Phase UPS. Gas-phase UPS of pentacene, **1**, and TIPS pentacene, **2**, allows comparison of the electronic properties of these pentacenes at the single molecule level (*intra*molecular properties). Detailed analyses of the gas-phase UPS and electronic structures of pentacene[13,31] and TIPS oligoacenes[30] have been reported previously. As shown in Figure 1, the TIPS group leads to the destabilization of the first ionization energy band of pentacene. The onset energy of the first ionization band, which is approximately the adiabatic ionization energy (AIE) for removal of an electron from the HOMO, is shifted 0.26 eV

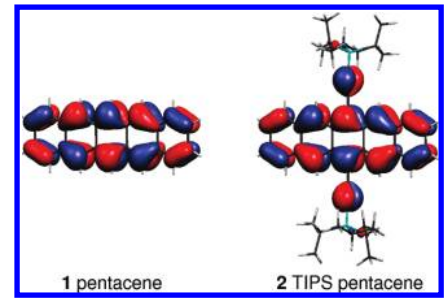

Figure 2. Highest occupied molecular orbitals of pentacene and TIPS pentacene.

to lower energy when pentacene is functionalized by the TIPS groups (see Experimental Details). This ionization energy shift is expected from simple orbital considerations because of the filled−filled interaction of the ethyne π-type HOMO electrons of the TIPS ethynyl groups with the π-type HOMO electrons of the pentacene core, shown in Figure 2. Computations show that the π-type orbital distribution of the pentacene core is delocalized with the TIPS substituents and results in a shift of the first ionization energy band to lower energy. From this gas phase trend in ionization energies of pentacene and TIPS pentacene, it is expected that the substitution of pentacene with TIPS groups will reduce the ionization energy in the solid. However, as we will demonstrate further, this ionization energy trend of pentacenes **1** and **2** in the gas phase is reversed in the solid phase.

Solid Phase UPS. The solid phase UPS measurements provide the ionization energies of molecules **1** and **2** in the presence of intermolecular interactions. These pentacenes were vapor deposited on a polycrystalline Au substrate. The subsequent depositions of 5 Å to 200 Å films of pentacene and of 10 Å to 200 Å films of TIPS pentacene on Au were studied by solid-phase UPS. We are interested in the properties of these films directly as deposited as in most device fabrications, and no attempts were made to increase crystallinity. The experimental setup with details is given below in the section "Experimental Details". The solid-phase ultraviolet photoelectron spectra of pentacene and TIPS pentacene films as a function of film thickness are shown in Figures 3 and 4, respectively. The high energy side of the photoelectron spectrum gives the value of the high binding energy cutoff (HBEC) of electron counts and the low energy side of the spectrum gives the first ionization energy band (the valence band) of the material. The HBEC of solid-phase UPS spectra was obtained as the cross point of the tangent to the high binding energy side with the baseline; the AIE was determined as the cross point of the tangent to the first IE band on the low energy side with the baseline. Energies from this experiment are reported to ± 0.1 eV. The HBEC shift (commonly termed the vacuum level shift) from Au to the organic layer signifies the presence of a strong interfacial dipole between Au and the organic layer, caused by the redistribution of electron density at the Au/organic layer interface.[14,37−41] The solid-phase photoelectron spectra

(33) Park, S. K.; Jackson, T. N.; Anthony, J. E.; Mourey, D. A. *Appl. Phys. Lett.* **2007**, *91*, 063514/1.
(34) Kim, D. H.; Lee, D. Y.; Lee, H. S.; Lee, W. H.; Kim, Y. H.; Han, J. I.; Cho, K. *Adv. Mater.* **2007**, *19*, 678.
(35) Landis, C. A.; Parkin, S. R.; Anthony, J. E. *Jpn. J. Appl. Phys.* **2005**, *44*, 3921.
(36) Northrop, B. H.; Houk, K. N.; Maliakal, A. *Photochem. Photobiol. Sci.* **2008**, *7*, 1463.
(37) Amy, F.; Chan, C.; Kahn, A. *Org. Electron.* **2005**, *6*, 85.
(38) Alloway, D. M.; Hofmann, M.; Smith, D. L.; Gruhn, N. E.; Graham, A. L.; Colorado, R., Jr.; Wysocki, V. H.; Lee, T. R.; Lee, P. A.; Armstrong, N. R. *J. Phys. Chem. B* **2003**, *107*, 11690.
(39) Cahen, D.; Kahn, A. *Adv. Mater.* **2003**, *15*, 271.
(40) Kang, S. J.; Yi, Y.; Kim, C. Y.; Cho, S. W.; Noh, M.; Jeong, K.; Whang, C. N. *Synth. Met.* **2006**, *156*, 32.

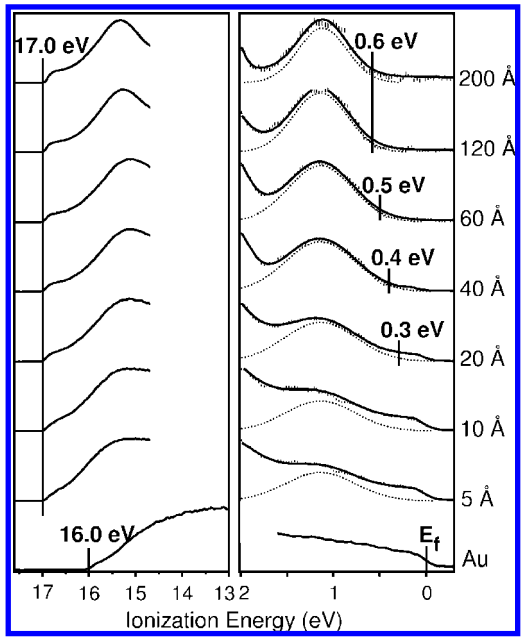

Figure 3. Solid-phase UPS of pentacene, **1**: the close up of the 1st ionization energy band (on the right); and the high binding energy cutoff (on the left) for 7 depositions.

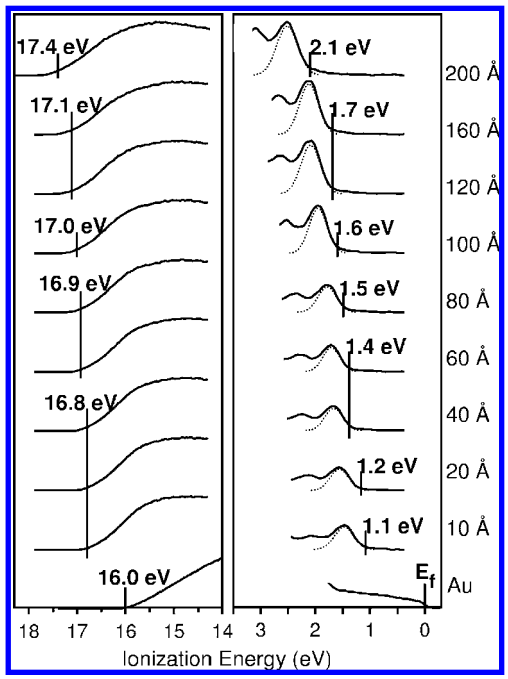

Figure 4. Solid-phase UPS of TIPS pentacene, **2**: the close up of the 1st ionization energy band (on the right) and the high binding energy cutoff (on the left) for 9 depositions.

of pentacene are in agreement with previously reported studies.[15,37,40–44] In the case of pentacene **1** (Figure 3), the HBEC shifts by 1.0 eV to the higher binding energy side for the first 5 Å coverage, and for thicker films the HBEC stays

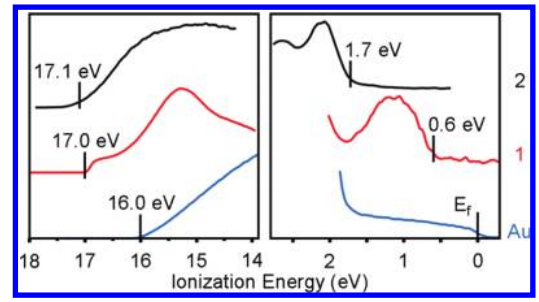

Figure 5. Solid phase He I UPS: on the right panel − first ionization energy bands of pentacene **1** (red), and of TIPS pentacene **2** (black), Fermi edge of Au (blue); on the left panel − high binding energy cutoffs of Au (blue), pentacene **1** (red), and TIPS pentacene **2** (black).

constant. In the case of TIPS pentacene **2** (Figure 4), the HBEC shifts from Au to a 10 Å film of **2** by 0.8 eV, and continues to shift slowly with increasing film thickness. This difference in behavior between TIPS pentacene and pentacene likely reflects the poorer charge transport behavior of the amorphous TIPS pentacene films compared to the pentacene films.

The HOMO level (AIE measured with respect to the Fermi energy of Au) of pentacene is observable but not accurately measured for the first two depositions due to the strong signal from Au. For films thicker than 10 Å the signal from pentacene increases, thus leading to a more pronounced valence band. Monitoring of the HOMO level and the HBEC with the thickness increase of pentacene indicates that the bulk properties of the film are achieved above 60 Å. The HOMO level of TIPS pentacene shifts gradually to the higher binding energy region; but for depositions above 100 Å and below 200 Å the HOMO level is stabilized with the corresponding stabilization of HBEC (±0.1 eV), meaning that within this thickness range the bulk properties of TIPS pentacene are achieved. The strong shift of the HOMO level and the HBEC of **2** observed for the 200 Å film indicates a charging effect which is an indicator of poor electron transfer through amorphous TIPS pentacene films.

We focus discussion on the bulk properties of molecules **1** and **2**. Pentacene and TIPS pentacene films of 120 Å thickness are presented in Figure 5. In the literature,[14,37,41,45,46] the hole-injection barrier (HIB) is defined as the AIE measured for the bulk sample with respect to the Fermi edge of clean Au, E_f. As can be seen from Figure 5, the HIB of pentacene **1** is 0.6 eV and that of TIPS pentacene **2** is 1.7 eV. The AIE measured with respect to the vacuum energy level, E_{vac} (discussed below), is 4.8 eV for **1** and 5.8 eV for **2**. By either method of energy referencing in the solid phase, the ionization energy and the hole-injection barrier of TIPS pentacene is greater than that of pentacene by 1.0 eV, which is a significant reversal of the order observed in the gas phase ionizations.

Figure 1 shows the relative ionization energies of both molecules in the gas phase and in the solid phase with the ionizations in both phases calibrated to the point of an electron with zero eV kinetic energy in vacuum, which corresponds by definition to ionization of an electron with a binding energy equal to the photon energy. It should be noted that the vacuum energy levels for the two experiments do not exactly coincide.[14]

(41) Schroeder, P. G.; France, C. B.; Park, J. B.; Parkinson, B. A. *J. Phys. Chem. B* **2003**, *107*, 2253.
(42) Fukagawa, H.; Yamane, H.; Kataoka, T.; Kera, S.; Nakamura, M.; Kudo, K.; Ueno, N. *Phys. Rev. B: Condens. Matter* **2006**, *73*, 245310/1.
(43) Sato, N.; Seki, K.; Inokuchi, H. *J. Chem. Soc., Faraday Trans. 2* **1981**, *77*, 1621.
(44) Sato, N.; Inokuchi, H.; Silinsh, E. A. *Chem. Phys.* **1987**, *115*, 269.
(45) Koch, N.; Kahn, A.; Ghijsen, J.; Pireaux, J.; Schwartz, J.; Johnson, R. L.; Elschner, A. *Appl. Phys. Lett.* **2003**, *82*, 70.
(46) Mori, T.; Fujikawa, H.; Tokito, S.; Taga, Y. *Appl. Phys. Lett.* **1998**, *73*, 2763.

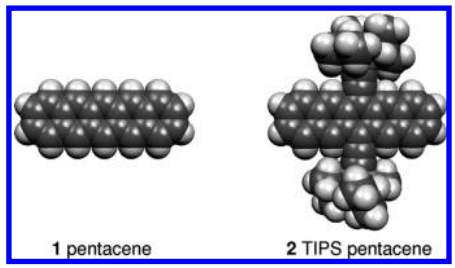

Figure 6. Space-filling models of pentacene **1** and TIPS pentacene **2**.

The vacuum level in the gas phase experiments corresponds to an absolute vacuum with the energies referenced to optical threshold ionizations,[47] in this case the argon $^2P_{3/2}$ ionization. The vacuum level in the solid phase experiments corresponds to the point of zero electron kinetic energy inside the instrument, identified in the experiment as the point of the high binding electron energy cutoff (HBEC) in Figure 5.[14] The similarity of the high binding energy cutoff values for the two molecules indicates that their surface dipoles and vacuum level reference energies are close to the same in the instrument. Figure 1 shows that on these scales the AIE of TIPS pentacene shifts 0.4 eV to lower ionization energy from the gas phase to the solid phase, while the AIE of pentacene shifts 1.7 eV to lower ionization energy. The lowering of the ionization energies from the gas phase to the solid phase is primarily due to the stabilization of the cations by polarization of the surrounding medium. The polarization energy has been defined in other works as the difference of AIE between the gas and solid phases,[43,44] but it should be remembered that this does not take into account the different vacuum levels mentioned above and other direct intermolecular interactions. The important point is that in going from the gas phase to the solid phase, the ionization energy of pentacene is lowered 1.3 eV more in energy than that of TIPS pentacene, and reverses the ionization order.

The relative stabilization of TIPS pentacene compared to pentacene with respect to electron loss follows from the different intermolecular electronic interactions in the solid phase. The situation is similar to the classic "anomalous" trend in the basicity of alkylamines from the gas phase to solution phase,[48−51] except that in this case, the property is a spectroscopic energy on the fast vertical time scale of ionization rather than a thermodynamic free energy that includes thermal and entropic effects and is on the slower time scale that allows molecular relaxation.[51] The difference in polarization of surrounding molecules in the bulk stabilizes the cation of pentacene more than the cation of TIPS pentacene, so that the ionization energy of pentacene is less than that of TIPS pentacene in the solid despite the fact that the HOMO of pentacene is more stable than the HOMO of TIPS pentacene in the neutral ground states of these molecules.

The origin of this difference in polarization can be understood from the structures of molecules **1** and **2** shown in Figure 6. Pentacene is significantly smaller in size than TIPS pentacene and allows closer contact of neighboring molecules to the acene core, even in a roughly amorphous state. TIPS pentacene on the other hand has the bulky TIPS groups, the triisopropylsilyl part of which already provides some polarization stabilization to the hole in the HOMO of the molecule cation in the gas phase (where the hole is delocalized with the ethynyl portion of the TIPS substituent, see Figure 2), and partially insulates the acene core from further interactions with neighboring molecules in the solid state. Thus the change in polarization stabilization of the positively charged acene core from the gas phase to the solid phase is expected to be less for TIPS pentacene than for pentacene. Also significant is the observation that the packing density of pentacene[52] (1.314 g/cm^3) is much greater than that of TIPS pentacene[1] (1.104 g/cm^3) despite the much heavier Si atoms in the latter molecule. Thus, the bulky TIPS groups in amorphous films significantly hinder tight three-dimensional packing, leading in turn to smaller polarization energy. Another indication of greater polarization effects in the pentacene films comes from the broader first ionization energy band of pentacene (by ∼0.3 eV) compared to that of TIPS pentacene. The larger polarization of the surrounding medium leads to larger intermolecular reorganization energy, which contributes to the width of the first IE band. The exact value of the intermolecular reorganization energy cannot be extracted from the width of the band due to other solid-state broadening effects,[43] but the trend in width of the ionization energy bands reflects the trend in intermolecular reorganization energies and in turn polarization energies.

As an aside, the single crystal structures of pentacene[52] and TIPS pentacene[1] are known to have different morphologies. The crystal structure of pentacene is characterized as a "herringbone" arrangement, whereas the crystal structure of TIPS pentacene is characterized by π-stacking in two dimensions with the TIPS groups separating the π stacks.[29] However, extensive π stacking in the amorphous TIPS pentacene films of this study is not expected as evidenced by the difference of optical-absorption spectra of amorphous and crystalline samples of TIPS pentacene.[53] The amorphous samples of TIPS pentacene do not show a red-shift in the absorption spectrum, whereas for crystalline films there is $a > 70$ nm red-shift attributed to extensive π stacking. But even if the amorphous TIPS pentacene films adopt some π-stacking arrangement on a small scale, the polarization stabilization that the TIPS pentacene cation experiences in the solid are still expected to be smaller than those of the pentacene cation. These molecules are not expected to be as polarizable in the π direction perpendicular to the plane of the molecule as in the longitudinal direction within the plane of the molecule. Therefore, the close contacts with edge-on orientations in the herringbone structure of pentacene are more conducive to polarization effects, and the TIPS group insulates from these interactions. Further experimental and theoretical study of crystalline films is warranted, but the trends observed for these amorphous films of pentacene and TIPS pentacene are also expected to be observed for crystalline films.

Solution Electrochemistry. Additional insight into the factors controlling the electronic properties of these molecules comes from measurement of the oxidation and reduction potentials of these molecules in solution. As mentioned above, an uncertainty in the solid thin film studies is the exact intermolecular arrangements around each molecule, and particularly the ques-

(47) Sansonetti, J. E.; Martin, W. C. *J. Phys. Chem. Ref. Data* **2005**, *34*, 1559.
(48) Brauman, J.; Riveros, J.; Blair, L. *J. Am. Chem. Soc.* **1971**, *93*, 3914.
(49) Aue, D.; Webb, H.; Bowers, M. *J. Am. Chem. Soc.* **1976**, *98*, 311.
(50) Aue, D.; Webb, H.; Bowers, M. *J. Am. Chem. Soc.* **1976**, *98*, 318.
(51) Caskey, D. C.; Damrauer, R.; McGoff, D. *J. Org. Chem.* **2002**, *67*, 5098.
(52) Campbell, R. B.; Robertson, J. M.; Trotter, J. *Acta Crystallogr.* **1961**, *14*, 705.
(53) Ostroverkhova, O.; Shcherbyna, S.; Cooke, D. G.; Egerton, R. F.; Hegmann, F. A.; Tykwinski, R. R.; Parkin, S. R.; Anthony, J. E. *J. Appl. Phys.* **2005**, *98*, 033701/1.

Table 1. Measured Adiabatic Ionization Energies (eV) and Electrochemical HOMO and LUMO (eV) Values of Pentacene (**1**) and TIPS Pentacene (**2**)

	gas phase	solution phase[b]			solid phase[c]	
molecule	AIE	HOMO	LUMO	gap	AIE	Δ_p[d]
1	6.54 (6.41)	−5.1 (−5.1)	−3.0 (−3.3)	2.1 (1.8)	4.81	1.73
2	6.28 (6.15)	−5.1 (−5.3)	−3.4 (−3.8)	1.7 (1.5)	5.84	0.44
shift	+0.26 (0.26)	0.0 (0.2)	0.4 (0.5)	0.4 (0.3)	−1.0	1.3

[a] Values from electronic structure calculations are in parentheses. See Supporting Information for computational details and uncertainties in measured values. [b] HOMO and LUMO values are obtained from redox potentials in *o*-dichlorobenzene relative to the absolute potential of Fc/Fc^+ (see Supporting Information). [c] Relative to instrument vacuum energy level. [d] Polarization energy defined as difference in gas and condensed phase AIEs.

tion of whether some local order around the molecules in the solid state is critical to the results. Such order does not exist in solution. In addition, the electrochemical measurements are thermodynamic quantities on a slower time scale compared to the spectroscopic UPS measurements on a fast time scale, so it is of interest to determine to what extent the trends observed in the solid carry over to the solution electrochemistry. The results are collected in Table 1 (see Experimental Details below). The similarity of oxidation potentials of **1** and **2** as well as the drastic difference of reduction potentials of these molecules are supported by a previous study.[36] Similar to the results from the solid phase UPS measurements, the stabilization of the pentacene cation in solution is greater than that of the TIPS pentacene cation in solution. In this case, the difference is about 0.3 eV, such that the potential for removal of an electron becomes about the same for these two molecules in solution, rather than the reversal observed in the solid phase study. The trend of greater stabilization of the pentacene cation compared to the TIPS pentacene cation in solution is the same as observed in the solid phase UPS, but to a smaller extent. It is not surprising that these molecules experience less different polarization effects in the solution phase compared with the solid state because both are in similar contact with the same solvent; the primary difference comes from the difference in the cavitation of the large TIPS pentacene versus the smaller unsubstituted pentacene. This result also suggests that the primary factor controlling the trend in relative stabilization is not the detailed explicit structure of the molecular environment, which is very different between the two phases, but depends to first order on the general properties of the environment, in this case the polarizability.

The shift in energy from the gas phase to the solution phase for removal of an electron from pentacene is 1.44 eV, and this value increases slightly to 1.7 eV from the gas phase to the solid. This supports the effective packing density and polarizability properties of the pentacene films discussed above. In contrast, the shift in energy from the gas phase to the solution phase from removal of an electron from TIPS pentacene is 1.18 eV, and this value decreases substantially to only 0.38 eV from gas phase to the solid. The amorphous TIPS pentacene films cannot achieve the packing density of the pentacene films and the polarizability properties are much less effective at stabilizing the cations. Nonetheless, in both solution and solid, the cations of TIPS pentacene experience less stabilization than the cations of pentacene.

Computations. Electronic structure computations support the principles revealed by these experiments. Explicit theoretical modeling of the solid state, which for polarization effects would require assumptions of intermolecular structures across many molecular dimensions, is beyond the scope of this contribution. However, the results above suggest that detailed structure is secondary to the governing principle of polarization stabilization, and implicit modeling of the trends in polarization effects is readily available with standard continuum solvation models. Emphasis is in modeling the solution oxidation potentials using methods that have been previously successful.[54,55] For the values reported here, calculations were performed as in the previous gas phase studies of these molecules[30] with the Amsterdam Density Functional program (see Supporting Information).[56−58] Ionization energies were obtained by ΔSCF calculations using the LDA VWN/TZ2P method. It has been reported previously that ΔSCF calculations for functionalized oligoacenes using the LDA VWN/TZ2P model reproduce the gas phase experimental results and trends very well.[30] Solution phase calculations were performed by applying the COSMO solvation model with dichlorobenzene as a solvent to the gas phase computations. In modeling the oxidation and reduction potentials, the thermal contributions to the *differences* in free energies between the neutral molecules and the ions are expected to be small because there is little change in mass between the neutral and the ions (one electron) and the reorganization energies are small with little change in structures and vibrational frequencies.[30] We have tested the sensitivity of the results to different density functionals, different Gaussian- and Slater-type basis sets, different solvation models, and different computational packages, and found similar trends in the ionization shifts and HOMO/LUMO gaps (see Supporting Information for details). As can be seen in Table 1, even the very basic implicit continuum model of electronic structure and polarization is able to account reasonably well for the trends in gas phase ionization energies and the relative shifts in solution phase oxidation potentials from the gas phase, in which the shift for pentacene is greater than that for TIPS pentacene, without explicit consideration of the structure of the molecular environment.

Energy Level Diagrams. Taking this information together allows construction of an approximate solid phase energy level diagram shown in Figure 7. The HOMO ionization energy levels are estimated from the AIEs measured in the solid state with respect to the Fermi level, E_f, of gold. In the solid phase the HOMO ionization energy of pentacene is smaller than that of TIPS pentacene by 1.1 eV. The LUMO energy levels with respect to the HOMO ionization energies are estimated in this diagram from the electrochemically measured HOMO−LUMO energy gaps.[59,60] The gap between the oxidation and reduction potentials of pentacene is measured to be 2.1 eV and that of TIPS pentacene is 1.7 eV (0.4 eV smaller, Table 1). This electrochemical estimate of the energy gap does not include

(54) Felton, G. A. N.; Vannucci, A. K.; Chen, J.; Lockett, L. T.; Okumura, N.; Petro, B. J.; Zakai, U. I.; Evans, D. H.; Glass, R. S.; Lichtenberger, D. L. *J. Am. Chem. Soc.* **2007**, *129*, 12521.
(55) Felton, G. A. N.; Vannucci, A. K.; Okumura, N.; Lockett, L. T.; Evans, D. H.; Glass, R. S.; Lichtenberger, D. L. *Organometallics* **2008**, *27*, 4671.
(56) Te Velde, G.; Bickelhaupt, F. M.; Baerends, E. J.; Fonseca Guerra, C.; Van Gisbergen, S. J. A.; Snijders, J. G.; Ziegler, T. *J. Comput. Chem.* **2001**, *22*, 931.
(57) Guerra, C. F.; Snijders, J. G.; Te Velde, G.; Baerends, E. J. *Theor. Chem. Acc.* **1998**, *99*, 391.
(58) ADF2006. 01d, *SCM, Theoretical Chemistry*; Vrije Universiteit: Amsterdam, The Netherlands, 2006.
(59) Silinsh, E. A.; Bouvet, M.; Simon, J. *Mol. Cryst. Liq. Cryst. Sci. Technol., Sect. C* **1995**, *5*, 1.
(60) Bouvet, M.; Silinsh, E. A.; Simon, J. *Mol. Cryst. Liq. Cryst. Sci. Technol., Sect. C* **1995**, *5*, 255.

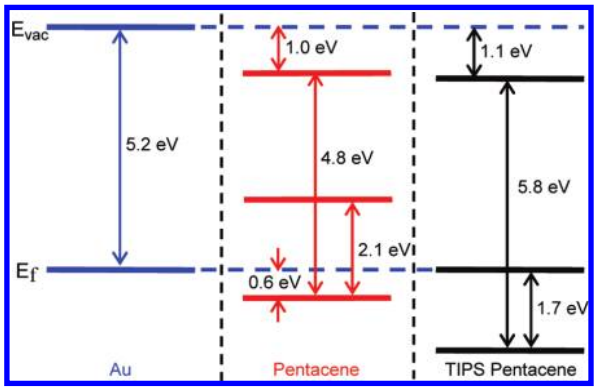

Figure 7. Solid phase energy level diagram of pentacene **1** and TIPS pentacene **2** with respect to a Au substrate.

the actual electronic interactions between molecules in the solid state and is considered an upper bound to the actual value. The solid-phase HOMO−LUMO energy gap also can be approximated by the optical energy gap, but in this case the exciton binding energy of the molecules is not accounted for.[41] The optical energy gap of pentacene is 1.8 eV[41,61] and that of TIPS pentacene is 1.6 eV[53] (0.2 eV smaller). According to both estimates, the energy gap of TIPS pentacene is smaller than that of pentacene. The smaller observed energy gap of TIPS pentacene is expected because of the greater conjugation in the TIPS pentacene molecule. As a consequence of both the trend in HOMO levels and the trend in HOMO−LUMO energy gaps seen in Figure 7, the LUMO energy level of TIPS pentacene is lower than the LUMO energy level of pentacene, thus leading to the smaller electron-injection barrier for TIPS pentacene vs that of pentacene (electron-injection barrier is defined as the position of LUMO level of the bulk sample with respect to the Fermi energy of clean gold[14,37,41,45,46]).

Conclusions

The combination of the gas-phase UPS, solid-phase UPS, and electrochemical measurements on these molecules illustrates an approach to the study of *intra-* and *inter*molecular electronic interactions. Each technique provides an energy measure of related processes, the removal of an electron from a molecule in the sample, under different circumstances. The relationships between the measurements allow the detailed understanding of electronic structure that is possible from experiments on molecules in the gas phase to be extended to the electronic properties in solution and the solid state. In the case of pentacene and TIPS pentacene, the electronic effects of the TIPS substituents on the ionization energies in the solid state are greater and in the opposite direction from the electronic effects on the ionization energies of the individual molecules in the gas phase. The change in polarization energy is likely to be a general factor for any material altered by the addition of insulating solubilizing substituents.

Experimental Section

Electrochemistry. Electrochemical data were measured using a BAS CV-50W voltammetric analyzer in a three cell configuration consisting of Ag wire pseudo reference electrode, platinum button as working electrode and platinum wire as counter electrode. Tetrabutylammonium hexafluorophosphate (TBAPF6) was dissolved in anhydrous *ortho*-dichlorobenzene (ODCB) to produce 0.1 M supporting electrolyte solution. Both cyclic voltammetry (CV) and differential pulse voltammetry (DPV) were performed for each acene. The system was calibrated versus the ferrocene/ferrocenium redox couple. To obtain the reductive electrochemistry of pentacene, the solutions were sparged with nitrogen for 5 min immediately prior to the analysis. A nitrogen blanket was also maintained above the solutions during the experiments. After the initial experiment, the solution was heated to encourage further dissolution of the pentacene analyte. The optimal potential window for both compounds was determined using CV, then the anodic and cathodic electrochemical processes were studied individually using DPV. Redox potentials were obtained from DPV experiments because DPV provides more reliable indications of HOMO and LUMO energy levels. The reduction and oxidation potentials of pentacene are −1.8 and 0.3 V respectively with respect to Fc/Fc^+. In the case of TIPS pentacene, the reduction potential is −1.4 V and the oxidation potential is 0.3 V. For CV we use a scan rate of 50 mV/s and for DPV 20 mV/s. These voltammetry experiments were used to obtain electrochemical HOMO−LUMO values and band gaps. Energies from electrochemistry measurements are reported to ± 0.05 eV. The observed potential values were then converted to vacuum energy levels according to literature methods.[62,63]

Gas-Phase Photoelectron Spectroscopy. The experiment setup details are given in Supporting Information. For the gas phase data analysis the two-mode Poisson vibrational progression fitting method was used to determine the vertical ionization (VIE) and reorganization energies (RE) of pentacene[13] and TIPS pentacene.[30] The AIE was obtained as the difference between the VIE and the RE. Due to the high sublimation temperature of both pentacenes hot bands were observed on the low energy side of the ionization band; the formation of these hot bands is caused by the thermal population of excited vibrational levels in the ground state of the neutral molecule, and therefore the onset of ionization intensity in the spectrum at this temperature does not signify the AIE. The presence of these hot bands was accounted for in the determination of the values of VIE, RE, and AIE. The arrows in Figure 1 are an approximate representation of the AIEs from this more detailed analysis. The uncertainties in the reported energies are on the order of ± 0.005 eV.

Solid-Phase Photoelectron Spectroscopy. The thin-film photoelectron spectra were collected at room temperature using a combined UPS-XPS Kratos Axis Ultra instrument with an average base pressure at or below 5×10^{-8} Torr, and the analyzer was operated in the constant analyzer energy (CAE) mode. UPS (valence) studies were performed using a gas discharge lamp (Omicrometer VUV Lamp HIS 13) producing He I (21.21 eV) photons, and the spectra were collected using a 5 eV pass energy. An accelerating bias voltage of 9 V was applied during the UPS data collection to improve the transmission of electrons with very low kinetic energy. XPS (core) studies were performed using a monochromatic Al Kα (1489 eV) excitation source, with pass energies of 20 eV for close-up spectra of the C 1s ionizations for **1**, and C 1s, Si 2p ionizations for **2**.

Thin-Film Preparation. Thin films of pentacene and TIPS pentacene were prepared by vapor deposition on a gold substrate in a UHV chamber connected to the UPS/XPS analysis chamber. Surface contaminants were removed from the polycrystalline gold foil prior to use by sputtering the surface with an argon ion beam set to 10−15 mA. The solid samples were placed into a boron nitride crucible and sublimed under vacuum (at or below 5.0×10^{-6} Torr) using a stainless steel Knudsen cell. A tantalum sleeve was attached to the top of the cell to help direct the sublimed sample to the substrate. Sublimation temperatures were monitored using a K-type thermocouple passed through an ultrahigh vacuum (UHV)

(61) Lee, J.; Hwang, D. K.; Park, C. H.; Kim, S. S.; Im, S. *Thin Solid Films* **2004**, *451−452*, 12.
(62) Li, Y.; Cao, Y.; Gao, J.; Wang, D.; Yu, G.; Heeger, A. J. *Synth. Met.* **1999**, *99*, 243.
(63) De Leeuw, D. M.; Simenon, M. M. J.; Brown, A. R.; Einerhand, R. E. F. *Synth. Met.* **1997**, *87*, 53.

feed and attached directly to the sample cell. Successive depositions were made at 220−240 °C for **1** and 275−295 °C for **2**. Film thicknesses were determined by monitoring the change in frequency of a quartz crystal microbalance (QCM) mounted parallel to the gold substrate in the deposition chamber. The change in frequency of 15 Hz corresponds to approximately 3 Å of each sample (a monolayer thickness), as also confirmed by attenuation of the Au $3d_{5/2}$ signal in the XPS spectrum. There were seven subsequent depositions of pentacene on Au made with thicknesses from 5 to 200 Å; there were nine depositions made of TIPS pentacene on Au with thicknesses from 10 Å to 200 Å. The deposition rate was 1 Hz per 1 s for both molecules. After each deposition of the sample, the UPS spectra were collected followed by the collection of XPS spectra. The film thickness of 120 Å was chosen for each sample for presentation in the discussion. At this film thickness, there was insignificant interfacial dipole formation observed, and also there was insignificant charging of the sample, as evidenced by the near constant position of the first ionization peak from 120−160 Å thicknesses for both samples. Above 160 Å thickness, the entire spectrum of the TIPS pentacene sample shifted substantially to higher energy with slight broadening of the first ionization band. However, for both samples the AIE remained constant within ± 0.1 eV relative to the high binding energy cutoff at all thicknesses.

Acknowledgment. Support from the National Science Foundation [CHE- 0749530 (Arizona) and CHE- 0749473 (Kentucky)] is gratefully acknowledged.

Supporting Information Available: Gas-phase UPS experimental details, computational details, and complete reference.[27] This material is available free of charge via the Internet at http://pubs.acs.org.

JA906917R